RESEARCH ARTICLE

Coordinating Bacterial Cell Division with Nutrient Availability: a Role for Glycolysis

Leigh G. Monahan,[a] Isabella V. Hajduk,[a] Sinead P. Blaber,[b] Ian G. Charles,[a] Elizabeth J. Harry[a]

The ithree institute, University of Technology, Sydney, New South Wales, Australia[a]; Department of Chemistry and Biomolecular Sciences, Macquarie University, North Ryde, New South Wales, Australia[b]

ABSTRACT **Cell division in bacteria is driven by a cytoskeletal ring structure, the Z ring, composed of polymers of the tubulin-like protein FtsZ. Z-ring formation must be tightly regulated to ensure faithful cell division, and several mechanisms that influence the positioning and timing of Z-ring assembly have been described. Another important but as yet poorly understood aspect of cell division regulation is the need to coordinate division with cell growth and nutrient availability. In this study, we demonstrated for the first time that cell division is intimately linked to central carbon metabolism in the model Gram-positive bacterium *Bacillus subtilis*. We showed that a deletion of the gene encoding pyruvate kinase (*pyk*), which produces pyruvate in the final reaction of glycolysis, rescues the assembly defect of a temperature-sensitive *ftsZ* mutant and has significant effects on Z-ring formation in wild-type *B. subtilis* cells. Addition of exogenous pyruvate restores normal division in the absence of the pyruvate kinase enzyme, implicating pyruvate as a key metabolite in the coordination of bacterial growth and division. Our results support a model in which pyruvate levels are coupled to Z-ring assembly via an enzyme that actually metabolizes pyruvate, the E1α subunit of pyruvate dehydrogenase. We have shown that this protein localizes over the nucleoid in a pyruvate-dependent manner and may stimulate more efficient Z-ring formation at the cell center under nutrient-rich conditions, when cells must divide more frequently.**

IMPORTANCE **How bacteria coordinate cell cycle processes with nutrient availability and growth is a fundamental yet unresolved question in microbiology. Recent breakthroughs have revealed that nutritional information can be transmitted directly from metabolic pathways to the cell cycle machinery and that this can serve as a mechanism for fine-tuning cell cycle processes in response to changes in environmental conditions. Here we identified a novel link between glycolysis and cell division in *Bacillus subtilis*. We showed that pyruvate, the final product of glycolysis, plays an important role in maintaining normal division. Nutrient-dependent changes in pyruvate levels affect the function of the cell division protein FtsZ, most likely by modifying the activity of an enzyme that metabolizes pyruvate, namely pyruvate dehydrogenase E1α. Ultimately this system may help to coordinate bacterial division with nutritional conditions to ensure the survival of newborn cells.**

Received 12 February 2014 **Accepted** 4 April 2014 **Published** 13 May 2014

Citation Monahan LG, Hajduk IV, Blaber SP, Charles IG, Harry EJ. 2014. Coordinating bacterial cell division with nutrient availability: a role for glycolysis. mBio 5(3):e00935-14. doi:10.1128/mBio.00935-14.

Editor Susan Gottesman, National Cancer Institute

Address correspondence to Elizabeth J. Harry, elizabeth.harry@uts.edu.au.

Cell division is fundamental to the survival and propagation of all living organisms. In bacteria, division is orchestrated by the highly conserved protein FtsZ, a tubulin-like GTPase (1–3). FtsZ initiates cell division by polymerizing into a ring structure (the Z ring) on the inner surface of the cytoplasmic membrane. The Z ring establishes the location of the division site, serves as a scaffold for the assembly of the division apparatus, and provides a contractile force to "pull in" the cell envelope during cytokinesis (4–7).

For division to produce viable daughter cells, it must be coordinated in time and space with the other major events of the cell cycle, such as chromosome replication and segregation. This is achieved through tight spatiotemporal regulation of Z-ring assembly. In well-studied rod-shaped bacteria, for example, the Z ring forms precisely at the cell midpoint and constricts between segregated chromosomes to generate identical progeny cells. Research into the control of Z-ring assembly has centered mainly on two regulatory systems, nucleoid occlusion and the Min system, which prevent Z rings forming at inappropriate positions in the cell (8–10). Nucleoid occlusion (11) blocks Z-ring formation over the nucleoid (chromosome) and is mediated by the DNA-binding proteins Noc in *Bacillus subtilis* (12) and SlmA in *Escherichia coli* (13). The Min system (14) consists of several proteins that prevent Z rings forming at the cell poles, where there is little or no DNA. The combined action of nucleoid occlusion and the Min system helps to ensure that Z-ring formation occurs efficiently and only at the cell center, although these systems are not responsible for actually identifying the midcell site, at least in *B. subtilis* (15). A number of additional proteins that bind to FtsZ and influence its polymerization *in vitro* and *in vivo* have been reported (2). The concerted activity of these proteins is thought to play a key role in regulating Z-ring assembly.

Another important and often overlooked aspect of cell division

and cell cycle control is the need to coordinate cell cycle events not only with one another but also with the growth rate and nutrient availability. Under nutrient-rich conditions, cells grow faster and thus double in mass more frequently. This must be accompanied by increases in the frequency of cell division, chromosome replication, and chromosome segregation while still maintaining proper coordination between these processes to ensure faithful cell proliferation (16, 17). Precisely how cell cycle dynamics are adjusted to compensate for changes in nutritional conditions is not well understood. However, recent breakthroughs in this area demonstrate that nutritional information can be transmitted directly from metabolic pathways to the cell cycle machinery and suggest that cell cycle processes may be continually fine-tuned via multiple signaling pathways that monitor the environment (18, 19).

A notable example is the nutrient-dependent regulation of bacterial cell size. It is well known that cell size increases in response to increases in nutrient availability (20–22), probably to accommodate the larger amounts of chromosomal DNA present at higher growth rates due to overlapping cycles of DNA replication (23). In a landmark study, Weart and colleagues (24) showed that nutrient-dependent changes in cell size are mediated by direct interaction between an enzyme in the glucolipid biosynthesis pathway (UgtP) and the cell division apparatus in *B. subtilis*. UgtP is able to detect nutrient levels via the accumulation of its substrate, the nucleotide sugar UDP-glucose. Following an increase in nutrient availability and a concomitant increase in the UDP-glucose concentration, UgtP interacts directly with FtsZ to delay cell division and increase cell size (24, 25). A similar UDP-glucose-dependent mechanism of cell size regulation has also been reported for *Escherichia coli* (26).

Importantly, UgtP-mediated inhibition of cell division is likely to occur only transiently after an elevation of nutrient levels (23). Once the correct cell size is achieved, division must not only resume but also take place more frequently to accommodate a now shorter mass doubling time. Together with the fact that *ugtP* mutants display no defects in growth, mass doubling time, or the timing of Z-ring assembly and constriction under steady-state conditions (24), this suggests that additional UgtP-independent mechanisms must exist to couple Z-ring formation and division with cell growth.

Here we have identified a new connection between cell division and glycolysis in *B. subtilis*. More specifically, we have shown that deletion of the gene encoding pyruvate kinase rescues the assembly defect of an *ftsZ* mutant and has profound effects on Z-ring formation in cells expressing wild-type *ftsZ*. These effects are the result of a disruption in pyruvate synthesis, and additional data suggest that the E1α subunit of pyruvate dehydrogenase may couple pyruvate production to Z-ring assembly via a novel moonlighting function. This is likely to play an important role in ensuring that bacterial division is properly coordinated with growth.

RESULTS

Inactivation of pyruvate kinase suppresses an *ftsZ* mutant. To identify proteins and pathways involved in the regulation of Z-ring assembly, we conducted a screen for extragenic suppressors of a temperature-sensitive *ftsZ* mutant of *B. subtilis*. The mutant, known as *ts*1, is incapable of dividing at high temperatures and grows into long, septumless filaments (27). This is caused by a single amino acid substitution at a conserved residue in FtsZ (28). At high temperatures, the mutant FtsZ(Ts1) protein is unable to support lateral interactions between polymer strands, which prevents it from forming a mature Z ring (29). Instead, FtsZ(Ts1) becomes trapped as a helical intermediate in the assembly pathway of the ring (28). Interestingly, this defect can be rescued by overproducing ZapA, an FtsZ binding protein that stimulates lateral FtsZ association (29). This indicates that it is possible to suppress the *ts*1 mutation by altering the balance of FtsZ regulatory proteins in the cell.

Using a transposon mutagenesis approach, we screened for Tn*10* insertions that restored viability to the *ts*1 strain at 48°C (see Materials and Methods). Although most previous studies have used 49°C as the nonpermissive temperature for *ts*1, we chose 48°C because we observed more robust and reproducible growth of suppressors at this temperature, with absolutely no growth for the *ts*1 parent (Fig. 1A). After screening ~10^6 CFU, we identified 5 that had stable suppressor mutations linked to a Tn*10* insertion. Sequencing the DNA flanking the transposon in each of these strains showed that two independent suppressors contained insertions in *pyk*, the gene encoding pyruvate kinase, while the other three were in unrelated genes.

Pyruvate kinase catalyzes the final reaction in glycolysis: the conversion of phosphoenolpyruvate to pyruvate. The pyruvate produced in this reaction can subsequently feed into the tricarboxylic acid (TCA) cycle or mixed acid fermentation or serve as a substrate for fatty acid and amino acid biosynthesis. Significantly, if the inactivation of *pyk* specifically rescues the *ts*1 mutant, this raises the possibility that there is a connection between glycolysis and cell division in bacteria. Three sets of data confirmed that the suppression of *ts*1 was specifically caused by inactivation of the *pyk* gene. First, we truncated *pyk* at the same site as the transposon (codon 270 of 585) using an insertion vector that places downstream genes under the IPTG (isopropyl-β-D-galactopyranoside)-inducible P_{spac} promoter. Viability was restored at 48°C in this strain (SU592), and this was unaffected by the presence or absence of the inducer, indicating that suppression is not due to effects on the expression of downstream genes (data not shown). In fact, *pyk* is predicted to be the final gene in a two-gene operon (30), making downstream effects unlikely. Second, we deleted the entire *pyk* open reading frame and found that this also suppressed the *ts*1 strain (Fig. 1Bi). Finally, we observed that the temperature-sensitive phenotype of *ts*1 was restored following complementation of *pyk* in *trans* under the xylose-inducible P_{xyl} promoter (Fig. 1B).

In restoring viability to the *ts*1 strain at the nonpermissive temperature, it was expected that *pyk* inactivation must rescue the ability of the mutant FtsZ(Ts1) protein to assemble into functional Z rings and support cell division. This was confirmed by microscopic analysis of *ts*1 cells harboring the *pyk* deletion (strain SU702) following growth at 48°C in liquid medium (L broth). First, while the *ts*1 parent strain (SU111) formed extremely long, septumless filaments at 48°C (average cell length of 32 ± 2 μm after 1 h of growth at 48°C) (Fig. 1C), SU702 cells were much shorter (6.1 ± 0.2 μm) and were often separated by clear gaps indicative of recently formed septa (Fig. 1D). In fact, SU702 cells were only slightly longer than wild-type cells (SU110) grown under the same conditions at 48°C (4.1 ± 0.1 μm) (Fig. 1E). This confirms that cell division is rescued in the absence of *pyk*. In addition, we used immunofluorescence microscopy to examine the localization of FtsZ(Ts1) and observed a striking rescue of

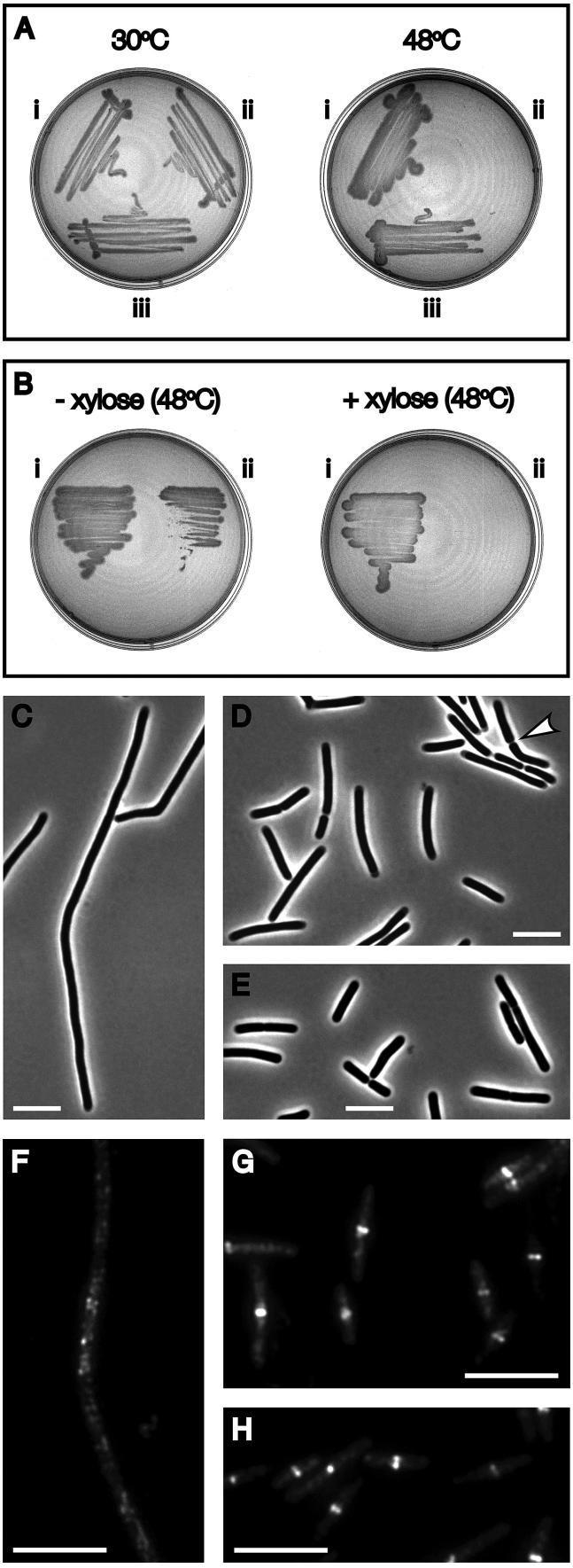

Z-ring formation in the *pyk* deletion strain (Fig. 1F to H). This indicates that the loss of pyruvate kinase restores activity to the FtsZ(Ts1) protein at 48°C.

Suppression of *ts*1 is not caused by growth effects or induction of stress responses. In addition to restoring viability to the *ts*1 strain at 48°C, the inactivation of *pyk* had a moderate effect on the growth rate. At 48°C, *ts*1 cells containing the *pyk* deletion exhibited a 1.4-fold increase in mass doubling time relative to that of the parent strain in L broth (~35 min versus ~25 min). A similar change in doubling time was also observed when the *pyk* deletion was introduced into wild-type *B. subtilis* cells, indicating that the growth defect is not specific to the *ts*1 mutant. Nonetheless, we performed a series of experiments to test whether the reduction in the growth rate was responsible for *ts*1 suppression and found that a decrease in the growth rate alone is not sufficient to rescue to rescue the *ts*1 mutation (see the supplemental material). We also observed that nutritional and energetic stress responses are not required for the suppression of *ts*1 (see the supplemental material).

Deletion of *pyk* affects Z-ring formation in wild-type cells. The above results raise the possibility that glycolysis, in particular pyruvate kinase, may be linked to the regulation of Z-ring formation in *B. subtilis*. If this is the case, we would expect the deletion of *pyk* to have some effect on Z-ring assembly in cells expressing the wild-type *ftsZ* gene. To test this, we examined the localization of FtsZ in cells with and without pyruvate kinase using a yellow fluorescent protein (YFP) tag. Strain SU679 (Δ*pyk*; FtsZ-YFP) was created for this purpose, harboring a xylose-inducible *ftsZ-yfp* gene fusion as well as the *pyk* deletion. Strain SU492 (FtsZ-YFP) served as an isogenic control for these experiments, containing only the *ftsZ-yfp* construct. In both strains, the *ftsZ-yfp* gene was inserted into the chromosome at the *amyE* locus in addition to the native copy of *ftsZ*. This construct has previously been shown to provide an accurate marker of FtsZ localization without affecting Z-ring assembly or division in wild-type *B. subtilis* cells (31–33).

Initially, both strains were grown in the presence of 0.01% xylose at 37°C, and cells were collected at mid-exponential phase for fluorescence visualization of FtsZ (Fig. 2). In the control strain (SU492), as expected, most cells (87%) contained a single Z ring positioned at the cell center (Fig. 2Aii), while all remaining cells lacked a visible Z ring. Interestingly, although the vast majority (86%) of *pyk* mutant (SU679) cells also contained Z rings, these rings were frequently found at positions close to the cell pole (32% of rings) (Fig. 2Bii [filled arrows]) as well as at the normal midcell

FIG 1 Inactivation of pyruvate kinase suppresses the *ts*1 mutant. (A) A transposon insertion in *pyk* restores viability to *ts*1 cells at 48°C. Strains were grown on tryptose blood agar plates at 30°C (permissive) or 48°C for 16 h. (i) Wild-type strain, SU110. (ii) *ts*1 (strain SU111). (iii) *ts*1 cells containing a suppressive transposon insertion in *pyk*. (B) Complementation of *pyk* restores the temperature-sensitive phenotype of *ts*1. Cells were grown in the presence or absence of 1% xylose for 16 h at 48°C. (i) Strain SU702 harboring the *ts*1 mutation and a deletion of the *pyk* gene. (ii) Strain SU610, in which *pyk* is expressed under xylose-inducible control at the ectopic *amyE* locus. (C to E) Deletion of *pyk* rescues *ts*1 cell division. Strains were grown in L broth for 1 h at 48°C and visualized by phase-contrast microscopy. (C) SU111 (*ts*1). (D) SU702 (*ts*1 Δ*pyk*). The arrow shows an example of a gap separating divided cells. (E) SU110 (wild type). (F to H) *pyk* deletion rescues Z-ring formation in *ts*1. FtsZ localization was visualized by immunofluorescence microscopy after growth for 1 h at 48°C. (F) SU111 (*ts*1), showing no Z rings. (G) SU702 (*ts*1 Δ*pyk*). Bright transverse bands represent normal-looking Z rings. (H) SU110 (wild type), showing normal Z rings at midcell. Scale bars, 5 μm.

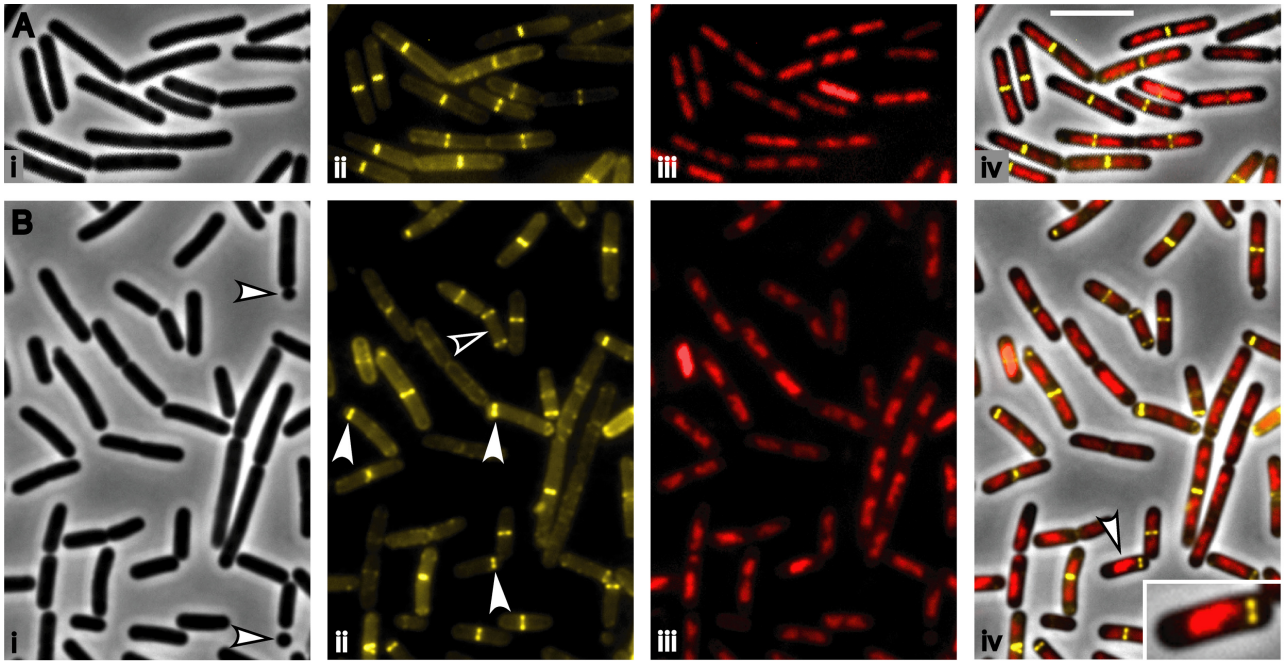

FIG 2 Deletion of *pyk* affects Z-ring formation in *B. subtilis*. SU492 (*amyE*::P_{xyl}-*ftsZ-yfp*) and SU679 (Δ*pyk amyE*::P_{xyl}-*ftsZ-yfp*) were grown to mid-exponential phase in the presence of 0.01% xylose at 37°C and visualized by phase-contrast and fluorescence microscopy. (A) SU492. (B) SU679. For both strains: i, phase-contrast image; ii, FtsZ-YFP localization, false colored in yellow; iii, DAPI staining of DNA, false colored in red; iv, overlay of panels i, ii, and iii. Arrows in panel Bi point to minicells. In panel Bii, filled arrows show examples of polar Z rings and the open arrow shows a cell with more than one ring. The arrow in Biv indicates a cell containing a polar Z ring and a single nucleoid with no visible evidence of segregation. The same cell is magnified in the inset. Scale bar, 5 μm.

site (68% of rings). In addition, ~6% of *pyk* mutant cells had more than one Z ring under these conditions, located at medial and/or polar positions (Fig. 2Bii [open arrow]). This resembles the phenotype of *B. subtilis* cells lacking the FtsZ regulatory proteins EzrA (34) and MinCD (35) and confirms that the deletion of pyruvate kinase has a genuine effect on Z-ring assembly.

The Z-ring positioning defect of the *pyk* mutant was not caused by a defect in the nucleoid occlusion system (see the introduction), since Z rings never formed directly over the chromosome in SU679 (Δ*pyk*; FtsZ-YFP) or SU492 (FtsZ-YFP) cells. Using the DNA stain DAPI (4′,6-diamidino-2-phenylindole) to covisualize FtsZ and the nucleoid, midcell Z rings were always observed between fully or partially segregated chromosomes in both strains, while polar Z rings in the *pyk* mutant were positioned adjacent to the nucleoid (Fig. 2). Moreover, the nucleoid localization pattern itself looked normal relative to that of the wild type in *pyk* mutant cells (with or without the FtsZ-YFP fusion), suggesting that the polar Z-ring phenotype is not caused by gross changes in the morphology, segregation, or positioning of the chromosome (Fig. 2Aiii and Biii).

Interestingly, it was found that at least some of the polar Z rings in the *pyk* mutant are able to support division, producing round "minicells" that lack chromosomal DNA. Minicells accounted for ~5% of the total population of SU679 (Δ*pyk*; FtsZ-YFP) cells in the presence of 0.01% xylose at 37°C (arrows in Fig. 2Bi), while no minicells were observed in the wild-type control (Fig. 2Ai). It is important to note that polar Z rings and minicells have also been reported in *B. subtilis* strains lacking the FtsZ inhibitors EzrA (34) and MinCD (35). However, unlike the case with pyruvate kinase, we previously showed that deletions in either *ezrA* or *minCD* do not rescue the FtsZ defect of the *ts*1 mutant (29). This strongly suggests that the *pyk* mutation does not affect Z-ring assembly via an effect on EzrA or MinCD activity but that it enables FtsZ to overcome the inhibitory action of these proteins at the cell pole.

Intriguingly, it also appears that polar Z rings can arise earlier in the cell cycle than normal medial rings in the *pyk* mutant. The average length of SU679 (Δ*pyk*; FtsZ-YFP) cells containing a single polar Z ring was significantly shorter than that of cells with a single Z ring at midcell (3.20 ± 0.03 μm versus 4.10 ± 0.05 μm; $P < 10^{-29}$), indicative of an earlier cell cycle stage. Moreover, some polar Z rings were observed in cells harboring a single-lobe nucleoid with no visible evidence of segregation (19% of SU679 cells containing a single polar ring) (Fig. 2Biv). In contrast, normal midcell Z rings formed only after visible chromosome segregation.

***pyk* mutant cells are hypersensitive to FtsZ overproduction.** In our initial experiments with the SU679 (Δ*pyk*; FtsZ-YFP) strain, the xylose-inducible FtsZ-YFP fusion protein was expressed via the addition of only 0.01% xylose to the growth medium. Interestingly, we found that production of higher levels of FtsZ-YFP greatly exacerbated the *pyk* mutant phenotype (Fig. 3). In the presence of 0.2% xylose, SU679 (Δ*pyk*; FtsZ-YFP) cells exhibited a much higher proportion of polar Z rings than in 0.01% xylose (52% of rings versus 32%; Fig. 3A and B). We also observed a 4-fold rise in the frequency of minicells in the population (22% versus 5%) and a 5-fold increase in the number of cells with multiple Z rings (32% versus 6%) under these conditions (Fig. 3A and B). In addition, the higher level of FtsZ-YFP resulted in the formation of a large number of aberrant, irregular FtsZ structures (arrows in Fig. 3A) that were never observed at low xylose concen-

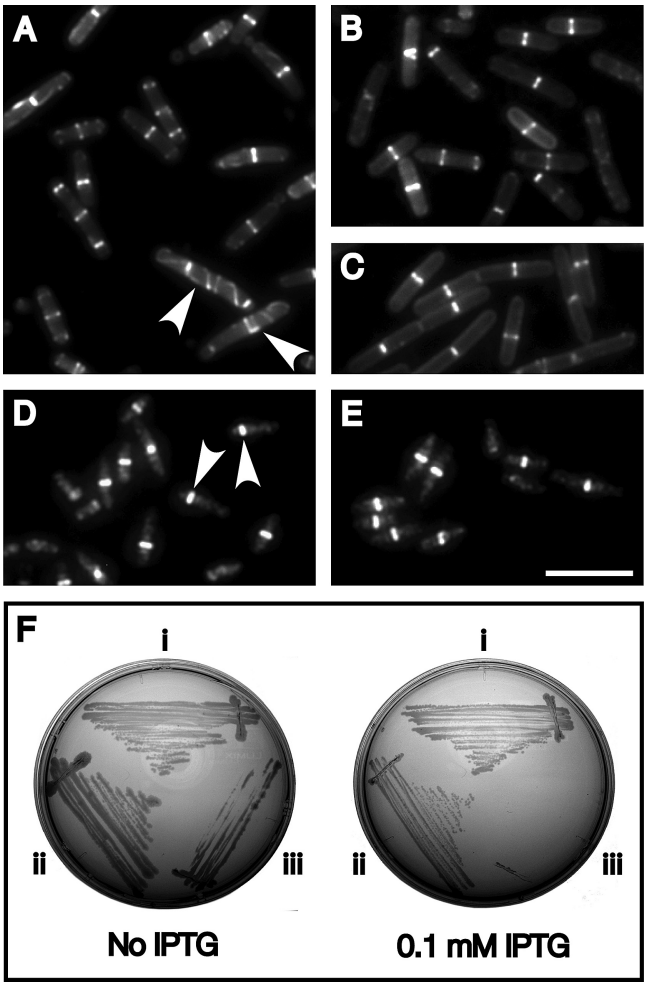

FIG 3 Deletion of *pyk* renders *B. subtilis* hypersensitive to FtsZ overproduction. Panels A to E show wild-type and *pyk* mutant cells expressing various levels of FtsZ-YFP in addition to the native FtsZ protein. Strains were grown to mid-exponential phase at 37°C, and FtsZ was detected by fluorescence visualization of FtsZ-YFP (A to C) or by immunofluorescence microscopy (D to E). (A) SU679 (Δ*pyk amyE*::P_{xyl}-*ftsZ-yfp*) expressing FtsZ-YFP in the presence of 0.2% xylose. Arrows indicate aberrant, irregular FtsZ structures. (B) SU679 cells in 0.01% xylose, showing a milder phenotype. (C) Control strain SU492 (*amyE*::P_{xyl}-*ftsZ-yfp*) showing normal midcell Z rings at the highest xylose concentration tested (0.2%). (D) Strain SU664 (Δ*pyk*), lacking FtsZ-YFP altogether. Arrows point to polar Z rings. (E) Isogenic wild-type strain SU5, showing normal midcell Z rings. Scale bar, 5 μm. (F) Overproduction of untagged FtsZ is lethal in the *pyk* mutant background. Cells were grown in the presence or absence of 0.1 mM IPTG for 16 h at 37°C. (i) Wild-type strain SU5; (ii) SU558 (*amyE*::P_{spachy}-*ftsZ*); (iii) SU696 (Δ*pyk amyE*::P_{spachy}-*ftsZ*).

trations (Fig. 3B) or in wild-type cells (Fig. 3C). Importantly, no differences in FtsZ localization whatsoever were detected in the wild-type control strain SU492 (FtsZ-YFP) at any xylose concentration (Fig. 3C). Moreover, quantitative Western blotting showed that there were no differences in the basal level of untagged FtsZ between wild-type and *pyk* mutant cells (data not shown). This suggests that the *pyk* mutant is hypersensitive to increases in the intracellular level of FtsZ (in the form of FtsZ-YFP).

In light of this result, we also examined FtsZ localization in *pyk* mutant cells lacking FtsZ-YFP by performing immunofluorescence microscopy with strain SU664 (Δ*pyk*). In SU664 (Δ*pyk*) cells, a significant number of Z rings (~15%) were positioned close to the cell pole (Fig. 3D). The SU664 (Δ*pyk*) strain also formed minicells, at a frequency of 1%, and an identical minicell frequency was observed for SU679 (Δ*pyk*; FtsZ-YFP) when grown without inducer. Importantly, these results confirm that there is a genuine Z-ring assembly defect in *pyk* mutant cells, even in the absence of FtsZ-YFP. However, this defect was more severe in cells expressing even low levels of FtsZ-YFP (see above), confirming that the *pyk* mutant phenotype is exacerbated by FtsZ-YFP production.

To determine whether the sensitivity to FtsZ-YFP was caused by the FtsZ moiety itself or the YFP tag, we overproduced untagged FtsZ by placing a second copy of the *ftsZ* gene at the *amyE* locus under the IPTG-inducible P_{spachy} promoter. FtsZ overproduction at high levels is known to be toxic in bacteria (36, 37). However, Δ*pyk* cells containing the P_{spachy}-*ftsZ* overexpression construct exhibited poor viability even in the presence of very low IPTG concentrations (between 0 and 0.01 mM), while IPTG levels above 0.01 mM eradicated growth altogether (Fig. 3F). In contrast, wild-type cells overexpressing *ftsZ* showed confluent growth for all IPTG concentrations up to 0.1 mM (Fig. 3F). FtsZ levels were equivalent between the wild-type and *pyk* mutant strains at each IPTG concentration (up to 0.01 mM), as demonstrated by Western blotting (data not shown). This confirms that the *pyk* mutant is hypersensitive to FtsZ overproduction, and it provides yet further evidence that the loss of pyruvate kinase interferes with normal Z-ring assembly in *B. subtilis*.

Proper Z-ring formation at midcell depends on the synthesis of pyruvate. While the data presented thus far indicate a link between glycolysis and cell division in *B. subtilis*, an important question remains: what is the molecular mechanism connecting these two pathways? More specifically, how exactly does the deletion of *pyk* lead to an effect on Z-ring formation? The simplest model is that the pyruvate kinase protein itself directly modulates FtsZ assembly *in vivo*, functioning as a negative regulator of Z-ring formation. In this model, the absence of pyruvate kinase would relieve an inhibition on FtsZ, which in the case of the FtsZ(Ts1) mutant would rescue Z-ring assembly. However, we were able to rule out this model by testing it using a combination of protein localization and protein-protein interaction techniques (see the supplemental material, including Fig. S1).

If pyruvate kinase does not regulate FtsZ assembly directly, we reasoned that the deletion of *pyk* may effect Z-ring formation by altering the expression/activity of another protein or metabolite in glycolysis or connected pathways. To narrow down where the connection to Z-ring assembly may lie, we screened a collection of metabolic mutants for their ability to rescue cell division and Z-ring formation in the *ts*1 strain at the nonpermissive temperature (Fig. 4). Mutations in 12 genes were tested (see Table S1 in the supplemental material for details of the mutations), including nine genes in central metabolic pathways (glycolysis and the TCA cycle) and three in the glucolipid biosynthesis pathway, which has a known additional role in coordinating cell size with nutrient availability (24). The functions of each gene are illustrated in Fig. 4A. Significantly, only 1 out of the 12 mutants tested (the *pgk* mutant) was found to rescue *ts*1 (Fig. 4B to E).

pgk encodes phosphoglycerate kinase, which converts 1,3-diphosphoglycerate to 3-phosphoglycerate during the final stages of glycolysis (Fig. 4). The phosphoglycerate kinase reaction is up-

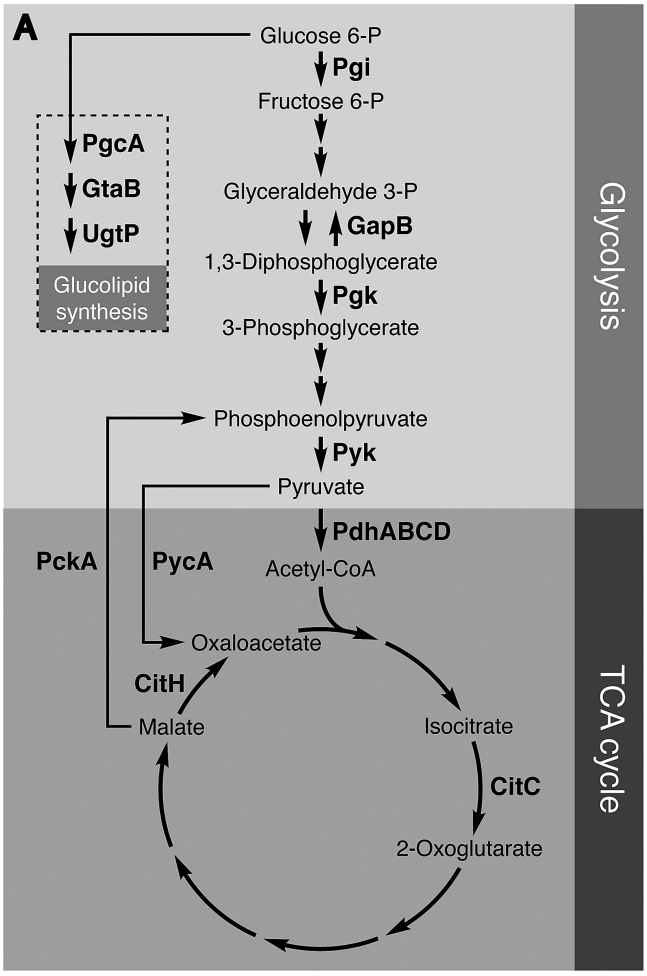

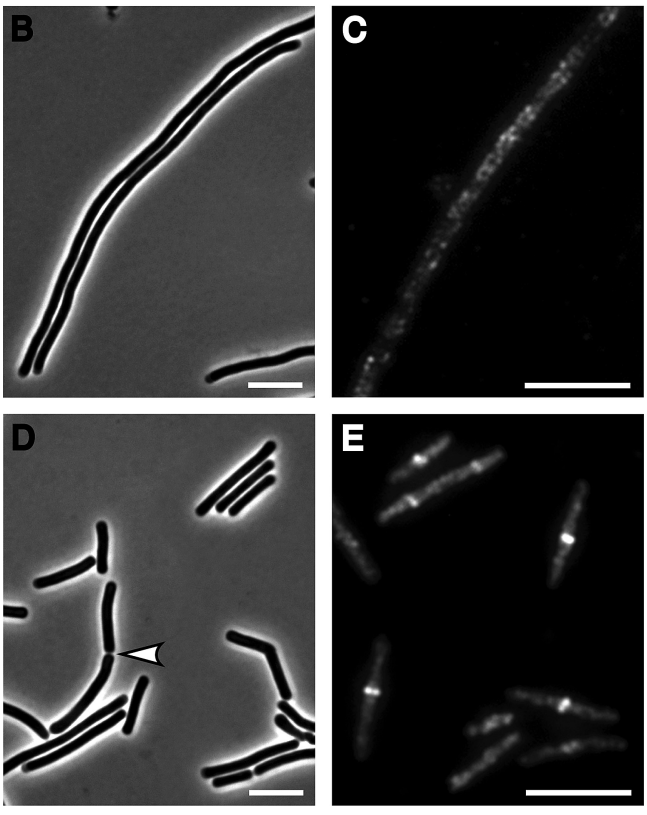

stream of pyruvate kinase, which argues that the effects of the *pyk* deletion on Z-ring formation are unlikely to be mediated by a buildup of the pyruvate kinase substrate phosphoenolpyruvate. Interestingly, as with pyruvate kinase, the phosphoglycerate kinase reaction is one of a series of reactions at the end of glycolysis that cannot be efficiently shunted by the pentose phosphate pathway and is therefore required for the normal synthesis of pyruvate via the glycolytic pathway. This raises the possibility that pyruvate itself is important for proper Z-ring formation and that it is the disruption of pyruvate production in the *pyk* mutant that affects FtsZ assembly.

To test this idea, we examined the effect of exogenous pyruvate on the *pyk* mutant phenotype. Strikingly, we found that the addition of 1% pyruvate to the growth medium (L broth) completely rescued the Z-ring assembly/positioning defect of the SU697 (Δ*pyk*; FtsZ-YFP) strain in the presence of 0.01% xylose at 37°C (Fig. 5). This rescue was also observed when we performed the experiment in a defined medium containing glucose as the sole carbon source, conditions under which it has been demonstrated experimentally that *B. subtilis pyk* mutants are deficient in producing endogenous pyruvate (38, 39; see also the supplemental material, including Fig. S2). Further to these experiments, we found that exogenous pyruvate overcomes the suppressive effects of a *pyk* deletion on the *ts*1 division mutant (see Fig. S3). Together these data suggest that pyruvate (or possibly a downstream metabolite) plays an important role in coordinating glycolysis with bacterial division. Moreover, these results further confirm that the metabolic connection to division is not mediated by pyruvate kinase directly, since it is possible to restore normal Z-ring formation in the complete absence of the pyruvate kinase enzyme simply by supplementing cells with the enzymatic product, pyruvate.

The E1α subunit of pyruvate dehydrogenase may couple pyruvate production with Z-ring formation. It is unlikely that pyruvate itself can directly modulate FtsZ assembly, since there is currently no evidence to suggest that pyruvate and FtsZ interact. However, pyruvate could regulate the activity of another protein that in turn effects Z-ring formation. To further probe the link between carbon metabolism and Z-ring assembly, we investigated the *in vivo* localization of a range of enzymes from glycolysis and

FIG 4 Effect of metabolic mutations on *ts*1 strain thermosensitivity. (A) Schematic representation of glycolysis, the TCA cycle, and the glucolipid biosynthesis pathway, highlighting 12 enzymes (bold) for which mutants were tested in this study. Pgi, phosphoglucose isomerase; GapB, glyceraldehyde-3-phosphate dehydrogenase; Pgk, phosphoglycerate kinase; Pyk, pyruvate kinase; PdhABCD, pyruvate dehydrogenase complex; CitC, isocitrate dehydrogenase; CitH, malate dehydrogenase; PckA, phosphoenolpyruvate carboxykinase; PycA, pyruvate carboxylase; PgcA, phosphoglucomutase; GtaB, uridine-diphosphoglucose pyrophosphorylase; UgtP, uridine-diphosphate glucosyltransferase. To assess the effect of metabolic mutations on the temperature-sensitive phenotype of *ts*1, each mutation was introduced into the *ts*1 genetic background, and the resulting strains (see Table S1 in the supplemental material) were grown for 1 h at 48°C. Cellular morphology was examined by phase-contrast microscopy, and FtsZ localization was visualized by immunofluorescence. (B) Phase-contrast image of strain SU703 (Δ*citC*), shown as a representative of 11 mutants that did not suppress *ts*1. SU703 formed long, septumless filaments identical to those of normal *ts*1 cells (see Fig. 1C). (C) FtsZ localization in SU703 (Δ*citC*), showing no Z rings. (D) Phase-contrast image of strain SU705, containing a suppressive mutation in *pgk*. SU705 cells were much shorter than those of the *ts*1 strain (7.5 ± 0.2 μm versus 33 ± 2 μm) and were often separated by clear gaps indicative of recently formed septa (one of these is highlighted by an arrow). (E) FtsZ localization in SU705, showing frequent Z rings. Scale bars, 5 μm.

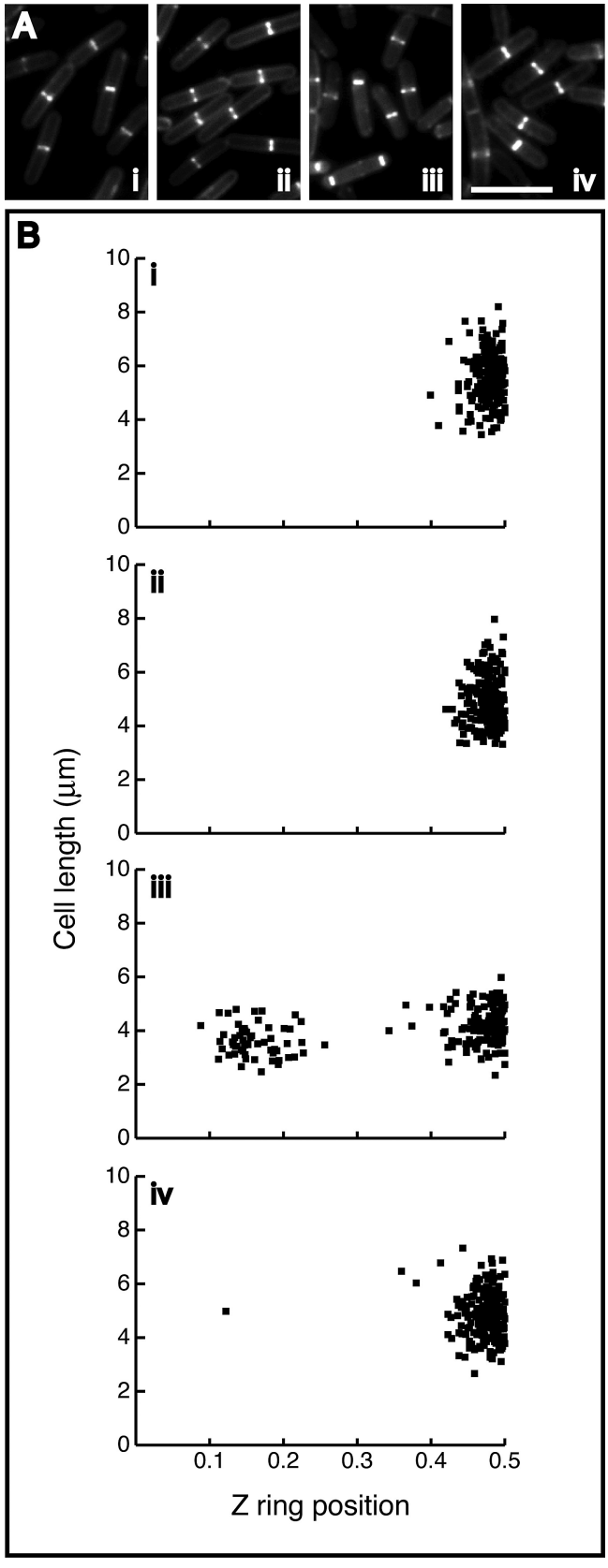

FIG 5 Addition of exogenous pyruvate rescues the Z-ring assembly defect of *pyk* mutant cells. SU492 (*amyE*::P_{xyl}-*ftsZ-yfp*) and SU679 (Δ*pyk amyE*::P_{xyl}-*ftsZ-yfp*) were grown to mid-exponential phase at 37°C in the presence of

(Continued)

connected pathways whose activity might be affected by the deletion of *pyk* and the disruption of pyruvate synthesis. Seven enzymes were chosen, including phosphoglycerate kinase (encoded by the *pgk* gene; see above) and two enzymes that utilize pyruvate as a substrate (pyruvate carboxylase [encoded by *pycA*] and the E1α subunit of pyruvate dehydrogenase [PDH] [encoded by *pdhA*]). Phosphoglucose isomerase (encoded by *pgi*), triose phosphate isomerase (encoded by *tpiA*), citrate synthase (encoded by *citZ*), and the pyruvate dehydrogenase E2 subunit (encoded by *pdhC*) were also tested. Importantly, all bacterial cell division and FtsZ regulatory proteins are known to exhibit a defined spatial pattern *in vivo*, most colocalizing with the Z ring (2, 40). Therefore, if any of these enzymes play a direct role in Z-ring assembly, one might expect a nonrandom localization pattern within the cell.

To test this, we constructed fluorescent protein fusions to each enzyme (see Materials and Methods) and visualized these in live cells grown to mid-exponential phase at 37°C. While six of the seven fusions localized homogenously throughout the cell, showing no evidence of foci or any form of specific spatial localization (data not shown), the E1α subunit of pyruvate dehydrogenase (PDH E1α) displayed an interesting localization pattern similar to that of the nucleoid (Fig. 6A). DAPI staining of cells expressing the PDH E1α-YFP fusion confirmed colocalization with the nucleoid (Fig. 6A). This spatial pattern is reminiscent of proteins involved in nucleoid occlusion, as well as other important cellular processes (see Discussion).

Intriguingly, when the PDH E1α-YFP fusion was expressed in a *pyk* mutant background, nucleoid colocalization was completely abolished (Fig. 6B). Instead, PDH E1α-YFP tended to accumulate in the nucleoid-free regions of the cell, particularly the cell poles (Fig. 6B). This polar localization pattern correlates with the polar Z-ring phenotype of *pyk* mutant cells. Moreover, the addition of 1% pyruvate to the growth medium, which rescues Z-ring formation to midcell in the *pyk* mutant, restored the nucleoid-like localization pattern of PDH E1α-YFP and prevented accumulation at the poles (Fig. 6C).

These results raise the possibility that PDH E1α functions as a nutrient-dependent regulator of Z-ring assembly whose activity and localization are controlled via the synthesis of pyruvate. Consistent with this idea, we observed that the localization of PDH E1α-YFP in wild-type *B. subtilis* cells varied with changes in nutrient conditions. In a minimal medium (SMM [Spizizen minimal medium] containing 1% glucose as the carbon source; see Materials and Methods), PDH E1α-YFP did not colocalize with the nucleoid as strongly as in rich broth, instead displaying a much more diffuse localization pattern throughout the cell (Fig. 6D). Areas of brighter PDH E1α-YFP signal could often be seen in regions occupied by the chromosome (arrows in Fig. 6D), imply-

Figure Legend Continued

0.01% xylose and the presence or absence of 1% sodium pyruvate. FtsZ localization was visualized by fluorescence microscopy, and Z-ring positioning was measured to illustrate the rescue of Z rings back to the cell center in the *pyk* mutant. Z-ring position was defined as the distance from the ring to the nearest pole divided by the cell length, such that a value of 0.5 corresponds to midcell and a value of 0 to the cell pole. (A) Fluorescence micrographs of FtsZ localization. (B) Scatter plots of Z-ring positioning. For both panels A and B: i, SU492 without added pyruvate; ii, SU492 in 1% pyruvate; iii, SU679 without pyruvate; iv, SU679 in 1% pyruvate. Scale bar, 5 μm.

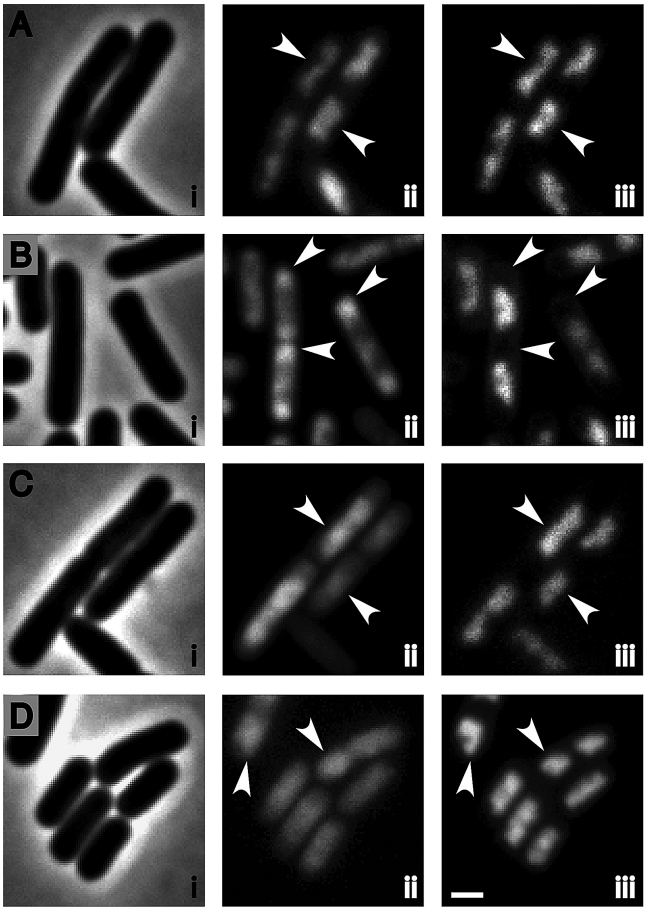

FIG 6 Localization of pyruvate dehydrogenase E1α in *B. subtilis*. Strains SU739 (*amyE*::P_{xyl}-*pdhA-yfp*) and SU742 (Δ*pyk amyE*::P_{xyl}-*pdhA-yfp*) were grown to mid-exponential phase at 37°C in the presence of 0.1% xylose and the presence or absence of 1% sodium pyruvate. PDH E1α-YFP (encoded by the xylose-inducible *pdhA-yfp* fusion gene) was visualized in live cells using fluorescence microscopy. (A) SU739 in L broth without added pyruvate. (B) SU742 in L broth without pyruvate. (C) SU742 in L broth with 1% pyruvate added. (D) SU739 in Spizizen minimal medium (SMM); no added pyruvate. For panels A to D: i, phase-contrast image; ii, PDH E1α-YFP localization; iii, DAPI staining of DNA. Arrows provide reference points for comparing PDH E1α and nucleoid localization patterns within the same cell. Scale bar, 1 μm.

ing that a low level of nucleoid association is still maintained under these conditions. Together the data suggest that PDH E1α exists in a nutrient-dependent equilibrium between nucleoid-associated and unassociated forms and that this equilibrium could be regulated through pyruvate levels. When pyruvate synthesis is artificially blocked by the deletion of pyruvate kinase, the equilibrium is shifted almost entirely to the unassociated form, and PDH E1α accumulates at the DNA-free cell poles.

Overproduction of PDH E1α exacerbates the polar Z-ring phenotype of *pyk* mutant cells. The observed correlation between PDH E1α localization and Z-ring position is consistent with a model in which PDH E1α can function either directly or indirectly as a positive regulator of FtsZ assembly. PDH E1α could help to stimulate Z-ring formation at midcell via its association with the nucleoid (see Discussion), while in *pyk* mutant cells, it could promote polar Z-ring assembly due to its own accumulation at the poles. If this model is correct, we hypothesized that it may be possible to increase the frequency of polar Z rings in cells lacking pyruvate kinase by producing higher levels of PDH E1α. To test this, we placed a second copy of the gene encoding PDH E1α (*pdhA*) under xylose-inducible control in the *pyk* mutant background (see Materials and Methods). We then induced PDH E1α overproduction by adding 1% xylose to the growth medium and examined FtsZ localization using immunofluorescence microscopy (see Fig. S4 in the supplemental material). Cells overproducing PDH E1α exhibited a statistically significant, 2.5-fold increase in the proportion of polar Z rings compared to that for an uninduced *pyk* mutant control (26% of rings versus 10.5%; see Fig. S4), consistent with a positive role for PDH E1α in Z-ring formation.

Combined loss of PDH E1α and FtsZ-binding protein EzrA results in a synthetic division defect. Overproduction of PDH E1α in wild-type *B. subtilis* cells did not significantly affect FtsZ localization under the conditions tested in our experiments (see Fig. S4 in the supplemental material). To further investigate whether PDH E1α plays a role in normal midcell Z-ring formation, it was important to examine the phenotype of cells lacking the enzyme. PDH E1α has previously been reported to be essential for viability in *B. subtilis* (41), and although we were able to construct a null mutation in *pdhA* quite readily (data not shown), colonies grew slowly and were likely to acquire suppressor mutations. For this reason, we decided to create a conditional mutant containing a single copy of *pdhA* under the xylose-inducible promoter, P_{xyl} (see Materials and Methods).

P_{xyl}-*pdhA* cells grown in the absence of xylose to deplete PDH E1α did not display any major defects in division or FtsZ assembly in a wild-type background (Fig. 7Aii and 7Bii). Similar observations have been reported for *B. subtilis* strains with null mutations in several FtsZ regulatory genes, such as *zapA* (42) and *sepF* (43, 44), due to redundancies within the network of proteins that control Z-ring formation. EzrA is another FtsZ-binding protein for which null mutants show only a mild division defect (slight increase in cell length, occasional minicells, and polar Z rings; Fig. 7; see also reference 34). However, cell division has been shown to be severely affected when an *ezrA* deletion is combined with mutations in other FtsZ regulatory genes, including both *zapA* (42) and *sepF* (43, 44). This suggests that *ezrA* mutants are sensitized to changes in the balance of FtsZ regulatory proteins.

To test whether the loss of PDH E1α affects cell division in an *ezrA* mutant background, we constructed strain SU792, containing a deletion of the *ezrA* gene and a xylose-inducible copy of *pdhA*. Significantly, the SU792 strain (Δ*ezrA* P_{xyl}-*pdhA*) exhibited major division defects when grown in the absence of inducer to deplete PDH E1α (Fig. 7). After depletion for 3 h, the average length of SU792 cells (10.1 ± 0.5 μm) was more than 2-fold greater than that for an SU792 control sample supplemented with xylose to maintain *pdhA* expression (4.8 ± 0.1 μm). Moreover, ~25% of the depleted cells were particularly filamentous under these conditions (11 to 46 μm) and were longer than any cells observed in populations lacking PDH E1α or EzrA alone (Fig. 7).

Using immunofluorescence microscopy, we also detected a striking defect in Z-ring formation in the PDH E1α-depleted, *ezrA* null cells. FtsZ localized at regular intervals along these cells, at positions corresponding to potential division sites. However, only 50% of localizations had the appearance of normal Z rings, with the remaining 50% comprised predominantly of short helix-like structures (see arrows in Fig. 7Bv). Interestingly, these helical assemblies closely resemble FtsZ structures that are observed tran-

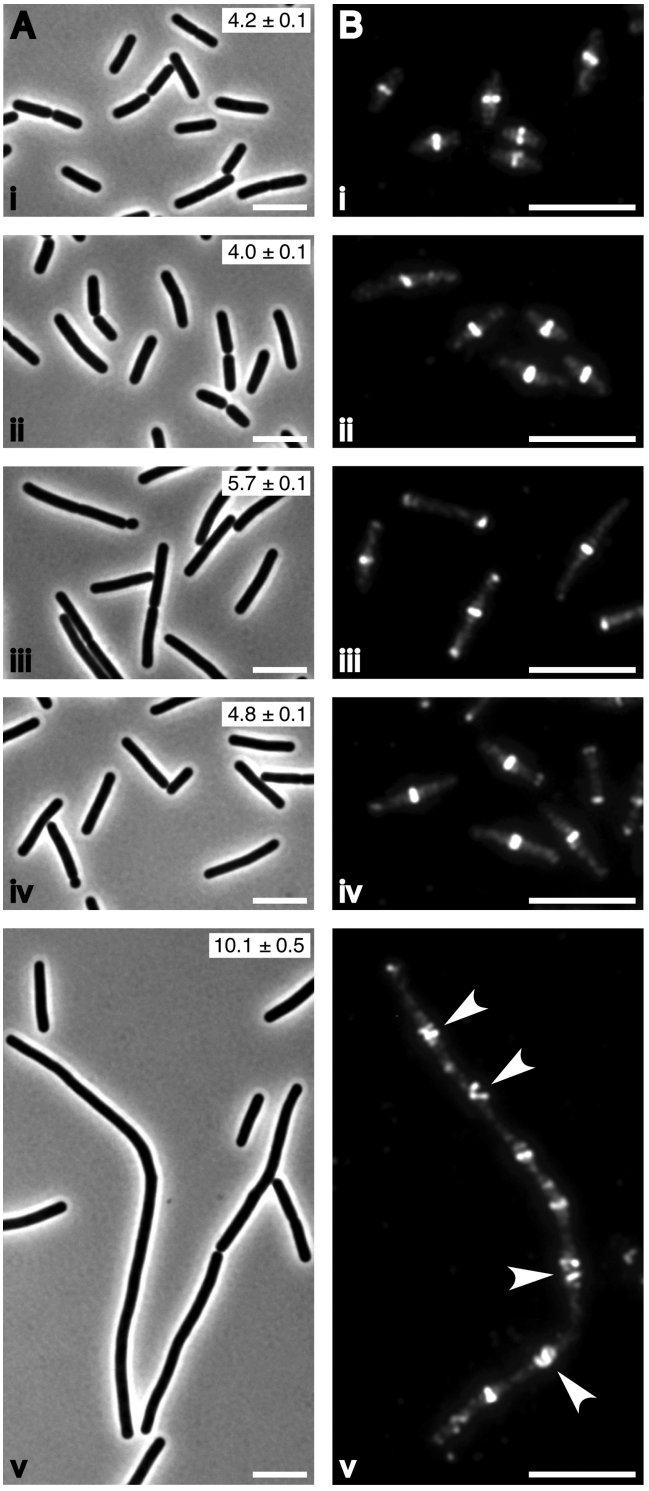

FIG 7 Depletion of PDH E1α affects Z-ring formation and cell division in a *B. subtilis ezrA* mutant. Cells were cultured in L broth to mid-exponential phase for 3 h at 37°C. Strains containing *pdhA* under xylose-inducible control were grown in the presence of 0.5% xylose to maintain *pdhA* expression or 1% glucose for maximal repression of the P_{xyl} promoter (83). It is important to note that 1% glucose or 0.5% xylose alone did not significantly affect division in wild-type cells (data not shown). Cellular morphology was examined by phase-contrast microscopy (A), and FtsZ localization was visualized by immunofluorescence (B). For both panels A and B: i, wild-type strain SU5; ii, strain SU791 (P_{xyl}-*pdhA*) supplemented with 1% glucose to deplete PDH E1α; iii, *(Continued)*

siently during the late stages of normal Z-ring formation in wild-type *B. subtilis* cells (31). This suggests that the normal pathway of Z-ring assembly may be delayed or inefficient in *ezrA* mutant cells lacking PDH E1α. Taken together, the results support the idea that PDH E1α plays a genuine role in *B. subtilis* Z-ring formation.

DISCUSSION

Faithful cell proliferation relies on the coordination of division with growth. Here we have shown that cell division is intimately linked to glycolysis in *B. subtilis*. Loss of pyruvate kinase disrupts this link and interferes with the normal function of the FtsZ protein and its assembly into the cytokinetic Z ring. A key component of the division/metabolism link is the synthesis of pyruvate, the product of the pyruvate kinase reaction. Addition of exogenous pyruvate restores normal division in a *pyk* mutant even in the absence of the pyruvate kinase enzyme itself. This connection between glycolysis and Z-ring formation is likely to play an important role in coordinating bacterial division with growth and nutrient availability.

Pyruvate is the end product of glycolysis and a key metabolite at the intersection of several important pathways. Accordingly, there are a number of potential fates for pyruvate *in vivo*. It can be used to generate energy and reducing power for the cell and also serves as a starting point for fatty acid biosynthesis and the production of several amino acids. Critically, the fate of pyruvate intimately depends on nutrient availability, since the pathways that metabolize it vary in activity with changes in nutrient levels (45). Any of these pathways could potentially connect to cell cycle processes, and it makes sense, therefore, that the cell might utilize pyruvate as a key component in mechanisms that coordinate division and the cell cycle with growth.

Our data suggest that pyruvate can influence cell division in *B. subtilis* through pyruvate dehydrogenase, a large multienzyme complex that links glycolysis with the TCA cycle by converting pyruvate to acetyl-coenzyme A (CoA). The pyruvate dehydrogenase complex consists of multiple copies of four subunits encoded by the *pdhABCD* operon (46, 47). Here we have shown that the E1α subunit, a product of the *pdhA* gene, likely plays a pyruvate-dependent role in the control of Z-ring assembly. Consistent with an FtsZ regulatory function, cells depleted of PDH E1α show major defects in division and Z-ring formation in a genetic background sensitized to changes in FtsZ regulation (Δ*ezrA*). In addition, the PDH E1α protein exhibits a nutrient-dependent localization pattern that is intimately linked to pyruvate synthesis. With increasing nutrient availability and rising pyruvate levels, it appears that an increasing proportion of PDH E1α molecules localize over the nucleoid. Conversely, when pyruvate synthesis is artificially blocked by the removal of pyruvate kinase, PDH E1α fails to associate with the nucleoid and accumulates at the DNA-free cell poles, where it may stimulate aberrant Z-ring assembly.

How does PDH E1α influence Z-ring formation in wild-type cells when localized over the chromosome? Interestingly, the proteins that mediate nucleoid occlusion, Noc in *B. subtilis* and SlmA

Figure Legend Continued

SU561 (Δ*ezrA*); iv, SU792 (Δ*ezrA* P_{xyl}-*pdhA*) in 0.5% xylose to maintain *pdhA* expression; v, SU792 (Δ*ezrA* P_{xyl}-*pdhA*) with PDH E1α depleted. Arrows indicate helix-like localizations of FtsZ. Numbers represent average cell lengths ± standard errors of the means. Scale bar, 5 μm.

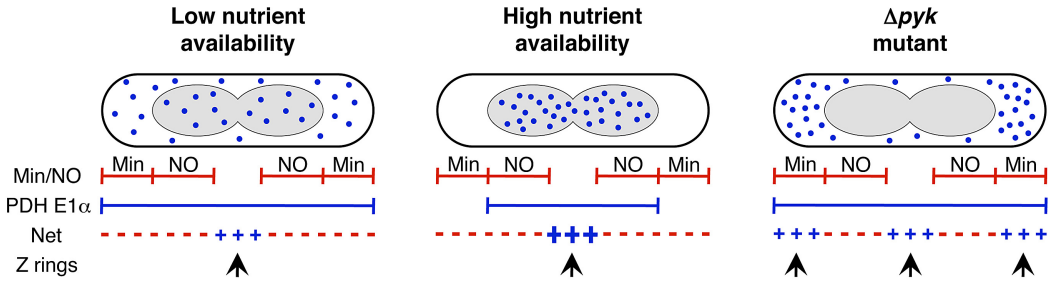

FIG 8 A nutrient-dependent role for PDH E1α in the control of Z-ring formation. Our results are consistent with a model in which PDH E1α (blue circles) acts as a positive regulator of FtsZ assembly and localizes over the nucleoid (gray) in a nutrient-dependent manner linked to pyruvate synthesis. PDH E1α exhibits only a weak association with the nucleoid under minimal-nutrient conditions (left), while in nutrient-rich media (center), it localizes much more strongly over the chromosome. Importantly, the negative regulatory systems Min and nucleoid occlusion (NO) are known to inhibit FtsZ polymerization at locations other than the cell center, and this could help to restrict the influence of PDH E1α on Z-ring formation to midcell. During the late stages of chromosome segregation (all cells are depicted at this point in the cell cycle), the proteins that mediate nucleoid occlusion are absent from the central region of the cell due to a lack of Noc/SlmA binding sites around the chromosome terminus. The amount of PDH E1α located within this central region increases with rising nutrient levels, and this could provide a positive signal for Z-ring formation at midcell that becomes stronger under nutrient-rich conditions (in which cells grow faster and must therefore divide more frequently). When pyruvate synthesis is artificially blocked in a *pyk* mutant, PDH E1α fails to colocalize with the nucleoid at all (right). Accumulation of PDH E1α at the nucleoid-free cell poles under these conditions could trigger polar Z-ring formation by overcoming the inhibitory effects of the Min system to generate a net positive signal for FtsZ assembly.

in *E. coli*, have been shown to bind specific DNA sequences that are particularly sparse or absent near the terminus region of the chromosome (48–50). It is thought that as the round of chromosome replication nears completion and the terminus region occupies a midcell location, Noc and SlmA move away from the midcell as the bulk of the chromosomes segregate, thus allowing Z-ring formation by relieving the inhibitory effects of nucleoid occlusion (48–50). It is possible that PDH E1α, via its association with the chromosome, actively promotes Z-ring formation in the central Noc/SlmA-free region of the cell during the late stages of chromosome segregation (Fig. 8). Importantly, this activity could be mediated by nutrient availability. More PDH E1α molecules localize over the nucleoid under nutrient-rich conditions, and this could promote more efficient Z-ring assembly in cells that need to divide more often due to a shorter mass doubling time (Fig. 8).

The idea that PDH E1α has a positive rather than inhibitory influence on FtsZ assembly is supported by several observations. For example, overproduction of PDH E1α in *pyk* mutant cells triggers an increase in the frequency of polar Z-ring formation. On the other hand, Z-ring assembly becomes less efficient in cells lacking PDH E1α (in combination with EzrA). A large proportion of FtsZ localizations are helical in nature under these conditions, raising the possibility that PDH E1α may help to stimulate the helix-to-ring remodeling of FtsZ polymers that occurs during normal Z-ring formation in *B. subtilis* (31). Intriguingly, similar helical FtsZ localization patterns have been observed in the *ts*1 division mutant and are caused by a defect in the bundling or lateral association of FtsZ protofilaments (28, 29). This defect can be suppressed by stimulating protofilament bundling (29), which suggests that PDH E1α may promote Z-ring formation/remodeling specifically by enhancing lateral FtsZ association. Whether PDH E1α binds FtsZ directly or via an interaction partner, for example, has yet to be determined.

A role for pyruvate dehydrogenase outside of metabolism is perhaps not surprising considering that there is a large and growing body of literature describing additional functions for many central metabolic enzymes (reviewed in references 51 to 55). These so-called "moonlighting" functions are widespread throughout nature, having been documented in bacteria through to humans. Moreover, moonlighting proteins are known to participate in a diverse and expanding range of processes, including transcriptional regulation, apoptosis, cell motility, and bacterial virulence. Intriguingly, an isoform of pyruvate kinase in mammals (PKM2) has been shown to play an important role in cancer cell proliferation (56), which is in part due to a nonmetabolic function as an activator of gene expression (57). Compounds that target PKM2 have recently been found to suppress tumor growth in mice, representing a promising avenue for the development of new anticancer drugs (58–60). Pyruvate kinase has also emerged as an excellent target for antistaphylococcal therapy (61), since the enzyme is essential for viability in *Staphylococcus aureus* (62) and has been shown to interact with a large number of diverse protein partners in this organism (63). In fact, several inhibitors of pyruvate kinase with potent activity against methicillin-resistant *S. aureus* strains have recently been described (61, 64–66).

In the present study, we demonstrated for the first time a tight connection between glycolysis and cell division in bacteria. Interestingly, previous reports for both *B. subtilis* (67) and *E. coli* (68) have identified a link between glycolysis and another major cell cycle process, chromosome replication. In the *B. subtilis* study, mutations in enzymes required for the terminal reactions of glycolysis were found to suppress conditional mutations in genes involved in the elongation or synthesis phase of DNA replication (67). Notably, these glycolytic mutations mapped to several genes, including both *pyk* and *pgk*, which we now have shown are linked to cell division. Given that DNA replication is itself intimately connected to the positioning of the division site in *B. subtilis* (69–71), it is tempting to speculate that all three processes, that is, glycolysis, chromosome replication, and cell division, may be tightly interconnected. Specifically, glycolysis could play an important role in coordinating replication with division by sensing nutrient levels and transmitting this information simultaneously to the division and replication machineries.

It is important to note that the effects of metabolic perturbations on Z-ring assembly described in this study do not appear to be caused by the disruption of a known DNA replication/division

link. This is because the previously reported role for chromosome replication in Z-ring positioning is specific to the initiation phase of replication (69–71), while the metabolic connection to replication is specific to the elongation or synthesis phase (67). In addition, we have observed that DNA replication initiation in *B. subtilis* is unaffected by the deletion of *pyk* (I. V. Hajduk, unpublished data). It is therefore likely that in *pyk* mutant cells, the early events of DNA replication can influence Z-ring assembly as normal.

How bacteria link cell cycle processes with growth is an intriguing and complex problem. We have now uncovered a new way in which this can occur. Further developments in this area will ultimately help us to understand, at a systems biology level, just how bacteria are able to faithfully and continually multiply in a constantly changing environment.

MATERIALS AND METHODS

General methods. Cloning and genetic manipulations were carried out using standard techniques (72, 73). *E. coli* strains DH5α (74) and C600 (75) were used for plasmid construction and propagation. Platinum *Pfx* (Invitrogen) or *Taq* (New England Biolabs) DNA polymerase was used for PCRs. *B. subtilis* chromosomal DNA was purified as described previously (76). DNA sequencing was performed by the Australian Genome Research Facility (Brisbane, Australia).

***B. subtilis* growth conditions.** *B. subtilis* strains were generally grown on tryptose blood agar plates or in L broth. Spizizen minimal medium (SMM) (77), containing 1% glucose or 1% monosodium succinate plus 0.2% monopotassium glutamate as the carbon source, was also used where specified. Media were supplemented with thymine (20 μg/ml) for strains harboring the *thyA* and *thyB* mutations (see Table S1 in the supplemental material). IPTG, xylose, sodium azide, DL-norvaline, or sodium pyruvate was added when required at appropriate concentrations. Antibiotics were used at the following concentrations: chloramphenicol, 5 μg/ml; erythromycin, 0.5 μg/ml; neomycin, 2.5 μg/ml; spectinomycin, 80 μg/ml; tetracycline, 12 μg/ml. Growth temperatures are specified above.

Strain construction. All *B. subtilis* strains used in this study are listed in Table S1 in the supplemental material. Details of strain construction are provided in the supplemental material.

Isolation and characterization of suppressors. Extragenic suppressors of the *ts*1 division mutant were isolated using the method of Weart et al. (78) with some modifications. Briefly, strain SU576 harboring the *ftsZ*(*ts*1) mutation and the thermosensitive transposon delivery plasmid pHV1249 (79) was first grown to early exponential phase (optical density at 600 nm [OD_{600}] of ~0.25) at 30°C in selective medium containing chloramphenicol. The culture was then diluted 2-fold in prewarmed medium at 51°C and grown for a further 2 h to select for loss of the plasmid and chromosomal integration of the transposon. Glycerol was added to a final concentration of 10%, and the culture was frozen in 1-ml aliquots at −80°C. Frozen aliquots were thawed and plated on selective medium at 48°C for selection of transposon insertions that restore viability to *ts*1 cells at the nonpermissive temperature. In addition, a small amount of thawed culture was serially diluted and grown at 30°C to determine the number of CFUs per ml of culture medium. A total of ~10^6 CFUs were screened over several experiments, and temperature-resistant colonies were obtained at a frequency of ~1 in 10^5. All suppressor isolates were replated on fresh medium at 48°C to verify the temperature resistance phenotype and checked for erythromycin sensitivity to confirm the loss of the plasmid backbone (79). Linkage of suppressor mutations to the transposon was demonstrated by transforming chromosomal DNA into a fresh *ts*1 background, selecting for chloramphenicol resistance, and screening for heat resistance.

To map the suppressor mutations onto the *B. subtilis* chromosome, the DNA flanking each transposon was first amplified by inverse PCR (80). This involved digesting genomic DNA from each suppressor strain with EcoRV, circularizing the resulting fragments by ligation, and selectively amplifying circular fragments that contain part of the transposon sequence using the primers 5′ GACTTACTCGTGGCTGCA 3′ and 5′ C CTAAGCGAACTGTTGAGAG 3′. PCR products were purified from agarose gel slices using the QIAquick gel extraction kit (Qiagen) and sequenced from the transposon edge into the surrounding DNA using the primer 5′ GACTTACTCGTGGCTGCA 3′. Sequence information was searched against the *B. subtilis* genome using the software program PSI-BLAST (81) (http://blast.ncbi.nlm.nih.gov/) to identify the exact location of the *ts*1 suppressor mutations on the chromosome.

Microscopy and image analysis. Samples were prepared for live cell fluorescence and immunofluorescence microscopy as described previously (29). For examination of cellular morphology and length, cells were fixed in 70% ethanol according to the method of Hauser and Errington (82). Samples were viewed using a Zeiss Axioplan 2 fluorescence microscope equipped with a 100× Plan ApoChromat phase-contrast objective (Zeiss) and an AxioCam MRm cooled charge-coupled-device (CCD) camera. Images were collected using the AxioVision software program, version 4.5 (Zeiss), and prepared for publication using the program Photoshop CS, version 8.0 (Adobe Systems). Cell length measurements were recorded using Axiovision (Zeiss), while statistical analysis was performed in the program Excel (Microsoft).

SUPPLEMENTAL MATERIAL

Supplemental material for this article may be found at http://mbio.asm.org/lookup/suppl/doi:10.1128/mBio.00935-14/-/DCSupplemental.

Text S1, DOC file, 0.1 MB.
Figure S1, TIF file, 2.2 MB.
Figure S2, TIF file, 2.1 MB.
Figure S3, TIF file, 2.5 MB.
Figure S4, TIF file, 2.5 MB.
Table S1, DOC file, 0.1 MB.

ACKNOWLEDGMENTS

We thank Petra Levin and Laurent Janniére for providing strains and protocols. We are also grateful to Abraham Sonenshein and Tom Ferenci for helpful discussions and critical reading of the manuscript.

This work was supported by an Australian Research Council Discovery project grant to E.J.H. (DP120102010). L.G.M. was supported by an ithree institute postdoctoral fellowship.

REFERENCES

1. **Harry E, Monahan L, Thompson L.** 2006. Bacterial cell division: the mechanism and its precision, p 27–94. *In* Jeon KW (ed), International review of cytology: a survey of cell biology, vol. **253**. Academic Press, San Diego, CA.
2. **Adams DW, Errington J.** 2009. Bacterial cell division: assembly, maintenance and disassembly of the Z ring. Nat. Rev. Microbiol. **7:**642–653. http://dx.doi.org/10.1038/nrmicro2198.
3. **de Boer PA.** 2010. Advances in understanding *E. coli* cell fission. Curr. Opin. Microbiol. **13:**730–737. http://dx.doi.org/10.1016/j.mib.2010.09.015.
4. **Erickson HP, Anderson DE, Osawa M.** 2010. FtsZ in bacterial cytokinesis: cytoskeleton and force generator all in one. Microbiol. Mol. Biol. Rev. **74:**504–528. http://dx.doi.org/10.1128/MMBR.00021-10.
5. **Osawa M, Anderson DE, Erickson HP.** 2008. Reconstitution of contractile FtsZ rings in liposomes. Science **320:**792–794. http://dx.doi.org/10.1126/science.1154520.
6. **Mingorance J, Rivas G, Vélez M, Gómez-Puertas P, Vicente M.** 2010. Strong FtsZ is with the force: mechanisms to constrict bacteria. Trends Microbiol. **18:**348–356. http://dx.doi.org/10.1016/j.tim.2010.06.001.
7. **Osawa M, Erickson HP.** 2013. Liposome division by a simple bacterial division machinery. Proc. Natl. Acad. Sci. U. S. A. **110:**11000–11004. http://dx.doi.org/10.1073/pnas.1222254110.
8. **Monahan LG, Liew ATF, Bottomley AL, Harry EJ.** 2014. Division site positioning in bacteria: one size does not fit all. Front. Microbiol. **5:**19. http://dx.doi.org/10.3389/fmicb.2014.00019.
9. **Bramkamp M, van Baarle S.** 2009. Division site selection in rod-shaped

bacteria. Curr. Opin. Microbiol. **12:**683–688. http://dx.doi.org/10.1016/j.mib.2009.10.002.
10. **Rothfield L, Taghbalout A, Shih YL.** 2005. Spatial control of bacterial division-site placement. Nat. Rev. Microbiol. **3:**959–968. http://dx.doi.org/10.1038/nrmicro1290.
11. **Wu LJ, Errington J.** 2011. Nucleoid occlusion and bacterial cell division. Nat. Rev. Microbiol. **10:**8–12. http://dx.doi.org/10.1038/nrmicro2671.
12. **Wu LJ, Errington J.** 2004. Coordination of cell division and chromosome segregation by a nucleoid occlusion protein in *Bacillus subtilis*. Cell **117:**915–925. http://dx.doi.org/10.1016/j.cell.2004.06.002.
13. **Bernhardt TG, de Boer PA.** 2005. SlmA, a nucleoid-associated, FtsZ binding protein required for blocking septal ring assembly over chromosomes in *Escherichia coli*. Mol. Cell **18:**555–564. http://dx.doi.org/10.1016/j.molcel.2005.04.012.
14. **Barak I.** 2013. Open questions about the function and evolution of bacterial Min systems. Front. Microbiol. **4:**378. http://dx.doi.org/10.3389/fmicb.2013.00378.
15. **Rodrigues CD, Harry EJ.** 2012. The Min system and nucleoid occlusion are not required for identifying the division site in *Bacillus subtilis* but ensure its efficient utilization. PLOS Genet. **8:**e1002561. http://dx.doi.org/10.1371/journal.pgen.1002561.
16. **Boye E, Nordström K.** 2003. Coupling the cell cycle to cell growth. EMBO Rep. **4:**757–760. http://dx.doi.org/10.1038/sj.embor.embor895.
17. **Cooper S, Helmstetter CE.** 1968. Chromosome replication and the division cycle of *Escherichia coli* B/r. J. Mol. Biol. **31:**519–540. http://dx.doi.org/10.1016/0022-2836(68)90425-7.
18. **Haeusser DP, Levin PA.** 2008. The great divide: coordinating cell cycle events during bacterial growth and division. Curr. Opin. Microbiol. **11:**94–99. http://dx.doi.org/10.1016/j.mib.2008.02.008.
19. **Wang JD, Levin PA.** 2009. Metabolism, cell growth and the bacterial cell cycle. Nat. Rev. Microbiol. **7:**822–827. http://dx.doi.org/10.1038/nrmicro2202.
20. **Schaechter M, Maaloe O, Kjeldgaard NO.** 1958. Dependency on medium and temperature of cell size and chemical composition during balanced growth of *Salmonella typhimurium*. J. Gen. Microbiol. **19:**592–606. http://dx.doi.org/10.1099/00221287-19-3-592.
21. **Sargent MG.** 1975. Control of cell length in *Bacillus subtilis*. J. Bacteriol. **123:**7–19.
22. **Donachie WD, Begg KJ.** 1989. Cell length, nucleoid separation, and cell division of rod-shaped and spherical cells of *Escherichia coli*. J. Bacteriol. **171:**4633–4639.
23. **Chien AC, Hill NS, Levin PA.** 2012. Cell size control in bacteria. Curr. Biol. **22:**R340–R349. http://dx.doi.org/10.1016/j.cub.2012.02.032.
24. **Weart RB, Lee AH, Chien AC, Haeusser DP, Hill NS, Levin PA.** 2007. A metabolic sensor governing cell size in bacteria. Cell **130:**335–347. http://dx.doi.org/10.1016/j.cell.2007.05.043.
25. **Chien AC, Zareh SK, Wang YM, Levin PA.** 2012. Changes in the oligomerization potential of the division inhibitor UgtP co-ordinate *Bacillus subtilis* cell size with nutrient availability. Mol. Microbiol. **86:**594–610. http://dx.doi.org/10.1111/mmi.12007.
26. **Hill NS, Buske PJ, Shi Y, Levin PA.** 2013. A moonlighting enzyme links *Escherichia coli* cell size with central metabolism. PLOS Genet. **9:**e1003663. http://dx.doi.org/10.1371/journal.pgen.1003663.
27. **Nukushina JI, Ikeda Y.** 1969. Genetic analysis of the developmental processes during germination and outgrowth of *Bacillus subtilis* spores with temperature-sensitive mutants. Genetics **63:**63–74.
28. **Michie KA, Monahan LG, Beech PL, Harry EJ.** 2006. Trapping of a spiral-like intermediate of the bacterial cytokinetic protein FtsZ. J. Bacteriol. **188:**1680–1690. http://dx.doi.org/10.1128/JB.188.5.1680-1690.2006.
29. **Monahan LG, Robinson A, Harry EJ.** 2009. Lateral FtsZ association and the assembly of the cytokinetic Z ring in bacteria. Mol. Microbiol. **74:**1004–1017. http://dx.doi.org/10.1111/j.1365-2958.2009.06914.x.
30. **Ludwig H, Homuth G, Schmalisch M, Dyka FM, Hecker M, Stülke J.** 2001. Transcription of glycolytic genes and operons in *Bacillus subtilis*: evidence for the presence of multiple levels of control of the *gapA* operon. Mol. Microbiol. **41:**409–422. http://dx.doi.org/10.1046/j.1365-2958.2001.02523.x.
31. **Peters PC, Migocki MD, Thoni C, Harry EJ.** 2007. A new assembly pathway for the cytokinetic Z ring from a dynamic helical structure in vegetatively growing cells of *Bacillus subtilis*. Mol. Microbiol. **64:**487–499. http://dx.doi.org/10.1111/j.1365-2958.2007.05673.x.
32. **Migocki MD, Lewis PJ, Wake RG, Harry EJ.** 2004. The midcell replication factory in *Bacillus subtilis* is highly mobile: implications for coordinating chromosome replication with other cell cycle events. Mol. Microbiol. **54:**452–463. http://dx.doi.org/10.1111/j.1365-2958.2004.04267.x.
33. **Migocki MD, Freeman MK, Wake RG, Harry EJ.** 2002. The Min system is not required for precise placement of the midcell Z ring in *Bacillus subtilis*. EMBO Rep. **3:**1163–1167. http://dx.doi.org/10.1093/embo-reports/kvf233.
34. **Levin PA, Kurtser IG, Grossman AD.** 1999. Identification and characterization of a negative regulator of FtsZ ring formation in *Bacillus subtilis*. Proc. Natl. Acad. Sci. U. S. A. **96:**9642–9647. http://dx.doi.org/10.1073/pnas.96.17.9642.
35. **Levin PA, Shim JJ, Grossman AD.** 1998. Effect of *minCD* on FtsZ ring position and polar septation in *Bacillus subtilis*. J. Bacteriol. **180:**6048–6051.
36. **Ward JE, Jr, Lutkenhaus J.** 1985. Overproduction of FtsZ induces minicell formation in *E. coli*. Cell **42:**941–949. http://dx.doi.org/10.1016/0092-8674(85)90290-9.
37. **Weart RB, Levin PA.** 2003. Growth rate-dependent regulation of medial FtsZ ring formation. J. Bacteriol. **185:**2826–2834. http://dx.doi.org/10.1128/JB.185.9.2826-2834.2003.
38. **Fry B, Zhu T, Domach MM, Koepsel RR, Phalakornkule C, Ataai MM.** 2000. Characterization of growth and acid formation in a *Bacillus subtilis* pyruvate kinase mutant. Appl. Environ. Microbiol. **66:**4045–4049. http://dx.doi.org/10.1128/AEM.66.9.4045-4049.2000.
39. **Pan Z, Zhu T, Domagalski N, Khan S, Koepsel RR, Domach MM, Ataai MM.** 2006. Regulating expression of pyruvate kinase in *Bacillus subtilis* for control of growth rate and formation of acidic byproducts. Biotechnol. Prog. **22:**1451–1455. http://dx.doi.org/10.1021/bp060049u.
40. **Errington J, Daniel RA, Scheffers DJ.** 2003. Cytokinesis in bacteria. Microbiol. Mol. Biol. Rev. **67:**52–65. http://dx.doi.org/10.1128/MMBR.67.1.52-65.2003.
41. **Gao H, Jiang X, Pogliano K, Aronson AI.** 2002. The E1beta and E2 subunits of the *Bacillus subtilis* pyruvate dehydrogenase complex are involved in regulation of sporulation. J. Bacteriol. **184:**2780–2788. http://dx.doi.org/10.1128/JB.184.10.2780-2788.2002.
42. **Gueiros-Filho FJ, Losick R.** 2002. A widely conserved bacterial cell division protein that promotes assembly of the tubulin-like protein FtsZ. Genes Dev. **16:**2544–2556. http://dx.doi.org/10.1101/gad.1014102.
43. **Ishikawa S, Kawai Y, Hiramatsu K, Kuwano M, Ogasawara N.** 2006. A new FtsZ-interacting protein, YlmF, complements the activity of FtsA during progression of cell division in *Bacillus subtilis*. Mol. Microbiol. **60:**1364–1380. http://dx.doi.org/10.1111/j.1365-2958.2006.05184.x.
44. **Hamoen LW, Meile JC, de Jong W, Noirot P, Errington J.** 2006. SepF, a novel FtsZ-interacting protein required for a late step in cell division. Mol. Microbiol. **59:**989–999. http://dx.doi.org/10.1111/j.1365-2958.2005.04987.x.
45. **Sonenshein AL.** 2007. Control of key metabolic intersections in *Bacillus subtilis*. Nat. Rev. Microbiol. **5:**917–927. http://dx.doi.org/10.1038/nrmicro1772.
46. **Neveling U, Bringer-Meyer S, Sahm H.** 1998. Gene and subunit organization of bacterial pyruvate dehydrogenase complexes. Biochim. Biophys. Acta **1385:**367–372. http://dx.doi.org/10.1016/S0167-4838(98)00080-6.
47. **Hemilä H, Palva A, Paulin L, Arvidson S, Palva I.** 1990. Secretory S complex of *Bacillus subtilis*: sequence analysis and identity to pyruvate dehydrogenase. J. Bacteriol. **172:**5052–5063.
48. **Cho H, McManus HR, Dove SL, Bernhardt TG.** 2011. Nucleoid occlusion factor SlmA is a DNA-activated FtsZ polymerization antagonist. Proc. Natl. Acad. Sci. U. S. A. **108:**3773–3778. http://dx.doi.org/10.1073/pnas.1018674108.
49. **Tonthat NK, Arold ST, Pickering BF, Van Dyke MW, Liang S, Lu Y, Beuria TK, Margolin W, Schumacher MA.** 2011. Molecular mechanism by which the nucleoid occlusion factor, SlmA, keeps cytokinesis in check. EMBO J. **30:**154–164. http://dx.doi.org/10.1038/emboj.2010.288.
50. **Wu LJ, Ishikawa S, Kawai Y, Oshima T, Ogasawara N, Errington J.** 2009. Noc protein binds to specific DNA sequences to coordinate cell division with chromosome segregation. EMBO J. **28:**1940–1952. http://dx.doi.org/10.1038/emboj.2009.144.
51. **Henderson B, Martin A.** 2013. Bacterial moonlighting proteins and bacterial virulence. Curr. Top. Microbiol. Immunol. **358:**155–213. http://dx.doi.org/10.1007/82_2011_188.
52. **Henderson B, Martin A.** 2011. Bacterial virulence in the moonlight: multitasking bacterial moonlighting proteins are virulence determinants in infectious disease. Infect. Immun. **79:**3476–3491. http://dx.doi.org/10.1128/IAI.00179-11.

53. **Copley SD.** 2012. Moonlighting is mainstream: paradigm adjustment required. Bioessays **34:**578–588. http://dx.doi.org/10.1002/bies.201100191.
54. **Huberts DH, van der Klei IJ.** 2010. Moonlighting proteins: an intriguing mode of multitasking. Biochim. Biophys. Acta **1803:**520–525. http://dx.doi.org/10.1016/j.bbamcr.2010.01.022.
55. **Kim JW, Dang CV.** 2005. Multifaceted roles of glycolytic enzymes. Trends Biochem. Sci. **30:**142–150. http://dx.doi.org/10.1016/j.tibs.2005.01.005.
56. **Christofk HR, Vander Heiden MG, Harris MH, Ramanathan A, Gerszten RE, Wei R, Fleming MD, Schreiber SL, Cantley LC.** 2008. The M2 splice isoform of pyruvate kinase is important for cancer metabolism and tumour growth. Nature **452:**230–233. http://dx.doi.org/10.1038/nature06734.
57. **Luo W, Hu H, Chang R, Zhong J, Knabel M, O'Meally R, Cole RN, Pandey A, Semenza GL.** 2011. Pyruvate kinase M2 is a PHD3-stimulated coactivator for hypoxia-inducible factor 1. Cell **145:**732–744. http://dx.doi.org/10.1016/j.cell.2011.03.054.
58. **Vander Heiden MG, Christofk HR, Schuman E, Subtelny AO, Sharfi H, Harlow EE, Xian J, Cantley LC.** 2010. Identification of small molecule inhibitors of pyruvate kinase M2. Biochem. Pharmacol. **79:**1118–1124. http://dx.doi.org/10.1016/j.bcp.2009.12.003.
59. **Anastasiou D, Yu Y, Israelsen WJ, Jiang JK, Boxer MB, Hong BS, Tempel W, Dimov S, Shen M, Jha A, Yang H, Mattaini KR, Metallo CM, Fiske BP, Courtney KD, Malstrom S, Khan TM, Kung C, Skoumbourdis AP, Veith H, Southall N, Walsh MJ, Brimacombe KR, Leister W, Lunt SY, Johnson ZR, Yen KE, Kunii K, Davidson SM, Christofk HR, Austin CP, Inglese J, Harris MH, Asara JM, Stephanopoulos G, Salituro FG, Jin S, Dang L, Auld DS, Park HW, Cantley LC, Thomas CJ, Vander Heiden MG.** 2012. Pyruvate kinase M2 activators promote tetramer formation and suppress tumorigenesis. Nat. Chem. Biol. **8:**839–847. http://dx.doi.org/10.1038/nchembio.1060.
60. **Goldberg MS, Sharp PA.** 2012. Pyruvate kinase M2-specific siRNA induces apoptosis and tumor regression. J. Exp. Med. **209:**217–224. http://dx.doi.org/10.1084/jem.20111487.
61. **Zoraghi R, See RH, Axerio-Cilies P, Kumar NS, Gong H, Moreau A, Hsing M, Kaur S, Swayze RD, Worrall L, Amandoron E, Lian T, Jackson L, Jiang J, Thorson L, Labriere C, Foster L, Brunham RC, McMaster WR, Finlay BB, Strynadka NC, Cherkasov A, Young RN, Reiner NE.** 2011. Identification of pyruvate kinase in methicillin-resistant *Staphylococcus aureus* as a novel antimicrobial drug target. Antimicrob. Agents Chemother. **55:**2042–2053. http://dx.doi.org/10.1128/AAC.01250-10.
62. **Zoraghi R, See RH, Gong H, Lian T, Swayze R, Finlay BB, Brunham RC, McMaster WR, Reiner NE.** 2010. Functional analysis, overexpression, and kinetic characterization of pyruvate kinase from methicillin-resistant *Staphylococcus aureus*. Biochemistry **49:**7733–7747. http://dx.doi.org/10.1021/bi100780t.
63. **Cherkasov A, Hsing M, Zoraghi R, Foster LJ, See RH, Stoynov N, Jiang J, Kaur S, Lian T, Jackson L, Gong H, Swayze R, Amandoron E, Hormozdiari F, Dao P, Sahinalp C, Santos-Filho O, Axerio-Cilies P, Byler K, McMaster WR, Brunham RC, Finlay BB, Reiner NE.** 2011. Mapping the protein interaction network in methicillin-resistant *Staphylococcus aureus*. J. Proteome Res. **10:**1139–1150. http://dx.doi.org/10.1021/pr100918u.
64. **Kumar NS, Amandoron EA, Cherkasov A, Finlay BB, Gong H, Jackson L, Kaur S, Lian T, Moreau A, Labrière C, Reiner NE, See RH, Strynadka NC, Thorson L, Wong EW, Worrall L, Zoraghi R, Young RN.** 2012. Optimization and structure-activity relationships of a series of potent inhibitors of methicillin-resistant *Staphylococcus aureus* (MRSA) pyruvate kinase as novel antimicrobial agents. Bioorg. Med. Chem. **20:**7069–7082. http://dx.doi.org/10.1016/j.bmc.2012.10.002.
65. **Axerio-Cilies P, See RH, Zoraghi R, Worral L, Lian T, Stoynov N, Jiang J, Kaur S, Jackson L, Gong H, Swayze R, Amandoron E, Kumar NS, Moreau A, Hsing M, Strynadka NC, McMaster WR, Finlay BB, Foster LJ, Young RN, Reiner NE, Cherkasov A.** 2012. Cheminformatics-driven discovery of selective, nanomolar inhibitors for staphylococcal pyruvate kinase. ACS Chem. Biol. **7:**350–359. http://dx.doi.org/10.1021/cb2003576.
66. **Zoraghi R, Worrall L, See RH, Strangman W, Popplewell WL, Gong H, Samaai T, Swayze RD, Kaur S, Vuckovic M, Finlay BB, Brunham RC, McMaster WR, Davies-Coleman MT, Strynadka NC, Andersen RJ, Reiner NE.** 2011. Methicillin-resistant *Staphylococcus aureus* (MRSA) pyruvate kinase as a target for bis-indole alkaloids with antibacterial activities. J. Biol. Chem. **286:**44716–44725. http://dx.doi.org/10.1074/jbc.M111.289033.
67. **Jannière L, Canceill D, Suski C, Kanga S, Dalmais B, Lestini R, Monnier AF, Chapuis J, Bolotin A, Titok M, Le Chatelier E, Ehrlich SD.** 2007. Genetic evidence for a link between glycolysis and DNA replication. PLoS One **2:**e447. http://dx.doi.org/10.1371/journal.pone.0000447.
68. **Maciąg M, Nowicki D, Janniere L, Szalewska-Pałasz A, Węgrzyn G.** 2011. Genetic response to metabolic fluctuations: correlation between central carbon metabolism and DNA replication in *Escherichia coli*. Microb. Cell Fact. **10:**19. http://dx.doi.org/10.1186/1475-2859-10-S1-S19.
69. **Regamey A, Harry EJ, Wake RG.** 2000. Midcell Z ring assembly in the absence of entry into the elongation phase of the round of replication in bacteria: co-ordinating chromosome replication with cell division. Mol. Microbiol. **38:**423–434. http://dx.doi.org/10.1046/j.1365-2958.2000.02130.x.
70. **Harry EJ, Rodwell J, Wake RG.** 1999. Co-ordinating DNA replication with cell division in bacteria: a link between the early stages of a round of replication and mid-cell Z ring assembly. Mol. Microbiol. **33:**33–40.
71. **Moriya S, Rashid RA, Rodrigues CD, Harry EJ.** 2010. Influence of the nucleoid and the early stages of DNA replication on positioning the division site in *Bacillus subtilis*. Mol. Microbiol. **76:**634–647. http://dx.doi.org/10.1111/j.1365-2958.2010.07102.x.
72. **Harwood CR, Cutting SM.** 1990. Molecular biological methods for Bacillus. John Wiley and Sons, Chichester, United Kingdom.
73. **Sambrook J, Russell DW.** 2001. Molecular cloning: a laboratory manual, 3rd ed. Cold Spring Harbor Laboratory Press, Cold Spring Harbor, NY.
74. **Hanahan D.** 1983. Studies on transformation of *Escherichia coli* with plasmids. J. Mol. Biol. **166:**557–580. http://dx.doi.org/10.1016/S0022-2836(83)80284-8.
75. **Jendrisak J, Young RA, Engel JD.** 1987. Cloning cDNA into lambda gt10 and gt11, p 359–370. *In* Berger SL, Kimmel AR (ed), Guide to molecular cloning techniques. Academic Press, San Diego, CA.
76. **Errington J.** 1984. Efficient *Bacillus subtilis* cloning system using bacteriophage vector phi 105J9. J. Gen. Microbiol. **130:**2615–2628.
77. **Anagnostopoulos C, Spizizen J.** 1961. Requirements for transformation in *Bacillus subtilis*. J. Bacteriol. **81:**741–746.
78. **Weart RB, Nakano S, Lane BE, Zuber P, Levin PA.** 2005. The ClpX chaperone modulates assembly of the tubulin-like protein FtsZ. Mol. Microbiol. **57:**238–249. http://dx.doi.org/10.1111/j.1365-2958.2005.04673.x.
79. **Petit MA, Bruand C, Jannière L, Ehrlich SD.** 1990. Tn10-derived transposons active in *Bacillus subtilis*. J. Bacteriol. **172:**6736–6740.
80. **Ochman H, Gerber AS, Hartl DL.** 1988. Genetic applications of an inverse polymerase chain reaction. Genetics **120:**621–623.
81. **Altschul SF, Madden TL, Schäffer AA, Zhang J, Zhang Z, Miller W, Lipman DJ.** 1997. Gapped BLAST and PSI-BLAST: a new generation of protein database search programs. Nucleic Acids Res. **25:**3389–3402. http://dx.doi.org/10.1093/nar/25.17.3389.
82. **Hauser PM, Errington J.** 1995. Characterization of cell cycle events during the onset of sporulation in *Bacillus subtilis*. J. Bacteriol. **177:**3923–3931.
83. **Kraus A, Hueck C, Gärtner D, Hillen W.** 1994. Catabolite repression of the *Bacillus subtilis xyl* operon involves a *cis* element functional in the context of an unrelated sequence, and glucose exerts additional *xylR*-dependent repression. J. Bacteriol. **176:**1738–1745.